



The detection of magnetotactic bacteria and magnetofossils by means of magnetic anisotropy

Andreas U. Gehring^{a,*}, Jessica Kind^a, Michalis Charilaou^a, Inés García-Rubio^b

^a Institute of Geophysics, ETH Zurich, 8092 Zurich, Switzerland

^b Laboratory of Physical Chemistry, ETH Zurich, 8093 Zurich, Switzerland

ARTICLE INFO

Article history:

Received 13 April 2011

Received in revised form 22 June 2011

Accepted 23 June 2011

Available online 14 July 2011

Editor: P. DeMenocal

Keywords:

ferromagnetic resonance spectroscopy (FMR)

Magnetospirillum gryphiswaldense

lake sediments

assembly of magnetosomes

cellular dipole

chain fragments

ABSTRACT

An important characteristic of magnetotactic bacteria (MTB) is the anisotropy of one-dimensionally aligned magnetite particles. This paper introduces the use of ferromagnetic resonance spectroscopy (FMR) at two different frequencies to compare the anisotropic properties of magnetite chains of cultured intact MTB with those of lake sediments of Holocene age in order to detect magnetofossils and to characterize their preservation in a geological system. Magnetite chains of intact MTB exhibit a predominantly uniaxial anisotropy. In the lake sediments, where diagenetic processes disintegrate the chains and diminish their uniaxiality, magnetite chains or chain fragments and dissociated bulk magnetite particles differ in their anisotropy properties. The two groups of assembly can be distinguished by empirical spectral separation of the FMR signal. This straightforward use of the characteristics of magnetic anisotropy provides a way to detect magnetofossils experimentally, thus allowing a better insight into microbial ecology during Earth's history.

© 2011 Elsevier B.V. All rights reserved.

1. Introduction

Since their discovery (Blakemore, 1975), there has been considerable interest in magnetotactic bacteria (MTB) and their fossil remains (magnetofossils) in geological systems as recorders of environmental conditions and of microbial ecology during Earth's history (Hesse, 1994; Kopp and Kirschvink, 2008). Moreover, magnetofossils are generally an ideal carrier of information of the Earth's magnetic field (Snowball and Sandgren, 2004). The hallmark of the MTB is their ability to form ferrimagnetic particles encapsulated in membranes termed magnetosomes, which can be stable in the geological time frame. These particles generally consist of stable single domain (SSD) magnetite (Fe_3O_4), with narrow size and shape distributions, organized in chains, stabilized by cytoskeletal protein filaments (Bazylinski and Frankel, 2004; Devouard et al., 1998; Muxworthy and Williams, 2009; Scheffel et al., 2006). The one-dimensional alignment of intracellular magnetic particles along their magnetic easy axes [111] generates a cellular magnetic dipole (Dunin-Borkowski et al., 1998; Frankel et al., 1979; Mann et al., 1987). This dipole enables the MTB to sense the geomagnetic fields and to direct their movement into favorable habitats (Bazylinski and Frankel,

2004). The proof that MTB inhabited ancient ecosystems can be complicated, because diagenetic processes lead to the decomposition of the cellular matter including the cytoskeletal protein filaments, which stabilize the magnetosome chains. Such decay diminishes the magnetic dipole of magnetite chains and consequently the uniaxiality. For the unequivocal identification of MTB, two criteria among others have to be fulfilled (e.g. Jimenez-Lopez et al., 2010; Kopp and Kirschvink, 2008). First, the magnetite particles must be in a SSD state; second, the particles must form one-dimensional assemblies with pronounced uniaxial anisotropy. The grain size criterion can be addressed by rock magnetic measurements such as hysteresis loops and remanence curves (Egli et al., 2010; McNeill and Kirschvink, 1993), whereas the anisotropy effect of the alignment of magnetite particles is more difficult to assess. Among the criteria for the detection of MTB, preserved magnetite chains are the most robust, because one-dimensional assembly of magnetite particles formed without an applied magnetic field is exclusively produced by MTB (Philippe and Maas, 2002; Zhang et al., 2009).

Ferromagnetic resonance (FMR) spectroscopy is a well-established way to analyze magnetic anisotropy (Bickford, 1950; Vonsovskii, 1966). Different responses of intact and lysed MTB to X-band FMR spectroscopy with microwave frequency in the 9 GHz-range provide compelling evidence that spectral traits (e.g. asymmetry of the absorption spectra) permit a direct way to detect the anisotropy of magnetosome chains (Fischer et al., 2008; Kopp et al., 2006b; Watanabe et al., 2009; Weiss et al., 2004). Furthermore, Mastrogiacomo et al. (2010) showed that

* Corresponding author.

E-mail addresses: agehring@erdw.ethz.ch (A.U. Gehring), jessica.kind@erdw.ethz.ch (J. Kind), michalis.charilaou@erdw.ethz.ch (M. Charilaou), garciarubio@phys.chem.ethz.ch (I. García-Rubio).

FMR experiments at different microwave frequencies can provide a more detailed insight into the anisotropy properties of magnetosomes chains.

In this paper we compare spectral traits obtained from intact cultured MTB and from Holocene lake sediment samples recorded at two different frequencies at room temperature. This new multiple-frequency approach offers a tool to test the robustness of magnetofossil detection by FMR spectroscopy and paves the avenue to decipher experimentally the evolution of magnetotactic microbes in a geological time frame.

2. Samples and methods

2.1. Laboratory grown MTB

Cultured *Magnetospirillum gryphiswaldense* strain MRS-1 was used as the reference for intact MTB (Fischer et al., 2008; Heyen and Schüler, 2003). This species forms magnetite with nearly equidimensional crystal morphology and a general grain size between 30 and 60 nm. In the mature state of *M. gryphiswaldense*, the magnetosomes are arranged like beads on a string. This alignment causes a cellular dipole with a pre-dominant uniaxial anisotropy (Faivre et al., 2010). For the magnetic investigation, the MTB were freeze-dried and sealed in paraffin in order to protect them from oxidation.

2.2. Natural sample

Sediments were analyzed from a piston core taken in a partly varved lake (Soppensee) in central Switzerland. This small lake covers an area of 0.227 km², and has neither an inflow nor an outflow, and, therefore, detrital input can be neglected (Fischer, 1996; Lotter, 2001). Three specimens (SOP_251, SOP_258, SOP_264) were sampled from a dark gray, organic-rich layer of about 40 cm in thickness. Sedimentological and paleoecological investigations showed that this layer formed under prevailing anoxic, non-sulfidic conditions during the Holocene (Lotter, 2001). Such a depositional environment is known to be likely a habitat for MTB (Snowball, 1994). The magnetic measurements of these lake sediments were performed on freeze-dried samples.

2.3. Static magnetic measurements

An alternating gradient magnetometer (Princeton Measurements Corporation) was used to measure the magnetic moments of the samples at room temperature. Magnetization loops were recorded while sweeping the external field in a range of ± 1 T. The measurements of three magnetization loops were averaged to obtain better statistics. The coercivity (B_c), the remanent magnetic moment (m_r), the saturation magnetic moment (m_s), and the saturation field (B_{sat}) were determined. The ratio of the remanent and saturation magnetization M_r/M_s was deduced from the ratio of the corresponding magnetic moments.

2.4. FMR spectroscopy measurements

In FMR experiments, the Larmor precessional motion of the magnetization in a magnetic field B is sustained by a perpendicularly incident microwave. Resonance occurs when the Larmor frequency of the magnetization tuned by an external field B_{ext} coincides with the microwave frequency and can be described as follows:

$$\hbar\nu = g \mu_B B_{res} \quad (1)$$

where \hbar is Planck's constant, ν is the microwave frequency, μ_B the Bohr magneton (9.274×10^{-24} Am²), g the spectroscopic splitting factor, which measures the energy splitting of degenerate states in a magnetic field, and B_{res} is the resonance field.

The B_{res} is the sum of B_{ext} and the internal field B_{int} . The latter contains different anisotropy contributions, such as magnetocrystalline and shape anisotropy. In systems with randomly oriented components, B_{int} cannot be measured directly. If the value of B_{ext} is plugged into the above resonance equation, an effective g -value, g_{eff} is obtained that takes into account the effect of B_{int} .

Magnetite particles in sediments or in MTB bulk samples are generally randomly oriented and each particle fulfills the resonance condition at a different B_{ext} , depending on its orientation. The observed spectrum arises from the sum of all resonances and B_{res} is defined as the value of the external field where the spectral absorption is maximum. The line-width ΔB , which depends on the total anisotropy, is defined as the full width at half the maximum (FWHM) amplitude of the absorption spectrum. The asymmetry parameter A is ascertained by the ratio of the high-field (ΔB_{high}) and the low-field (ΔB_{low}) parts of the absorption peak at FWHM (Faivre et al., 2010; Kopp et al., 2006a).

Spherical SSD magnetite particles exhibit isotropic spectra with $A \approx 1$. Randomly interacting SSD particles have $A > 1$ (i.e. $\Delta B_{low} < \Delta B_{high}$) and the B_{res} is shifted to lower fields with correspondingly higher g_{eff} (Valstyn et al., 1962). An opposite shift with $A < 1$ ($\Delta B_{low} > \Delta B_{high}$) is observed for interacting SSD magnetite in MTB where the particles aligned in chains, and generate cellular magnetic dipoles with pronounced uniaxiality (Faivre et al., 2010; Kopp et al., 2006b).

According to the equation above, the resonance field B_{res} depends on the microwave frequency. In this study X- and S-band FMR spectroscopy are used with microwave frequencies of 9.81 GHz and 4.02 GHz, respectively. An important difference of the two FMR setups is that in the S-band the resonance condition for one-dimensional assemblies of magnetite can be fulfilled if $B_{res} < B_{sat}$.

Freeze-dried magnetotactic bacteria and lake sediments fixed in ESR quartz glass tubes were used for S- and X-band measurements. First derivative X-band spectra were recorded on a Bruker EMX spectrometer operating at a microwave frequency of 9.81 GHz, with a power of 0.06 mW, modulation amplitude of 0.1 mT, and a modulation frequency of 100 kHz. The S-band FMR spectra were measured on a custom-built spectrometer controlled by Spec-Man software operating at a microwave frequency of 4.02 GHz, power of 2 mW and modulation amplitude of 0.1 mT.

In addition to the experiments, an analytical derivation of the FMR spectra is used following the model by Charilaou et al. (2011). In the case of intact MTB with uniform shape distribution, the magnetic anisotropy can be calculated exactly and be used to simulate FMR signals of randomly oriented MTB ensembles. In a first analytical approach by Kopp et al. (2006a,b) FMR spectra from intact MTB were simulated by an approximation using uniaxial shape anisotropy or cubic anisotropy of magnetite. Charilaou et al. (2011) showed that a magnetite chain can be modeled as a rotation ellipsoid with both uniaxial shape and cubic anisotropy for magnetite. In their holistic approach the two anisotropy contributions make up the sum of magnetic anisotropy for MTB and can be described using a uniaxial field B_{uni} and a cubic field B_{cub} (for magnetite B_{cub} is defined as $K_1/M = -23.5$ mT for $M = 470$ emu/cm³). Taking these anisotropy fields, the resonance condition can be obtained which is then used to calculate the resonance field B_{res} in equilibrium at each orientation of the external field. In order to simulate FMR spectra the resonance field of each orientation is employed to generate Gaussian curves. Finally all FMR spectra are superimposed to compile the net FMR signal for an ensemble of randomly oriented MTB. In a saturated state, where the condition $B_{res} > B_{sat}$ is fulfilled the superposition of signals has to be weighted statistically. This weighting describes the probability $p(\theta_B)$ of finding a chain oriented in the direction of the external field:

$$p(\theta_B) = \frac{\sin^2(\theta_B)}{4\pi^2} \quad (2)$$

where θ_B is the polar angle of the external field (in spherical coordinates). With this in mind, this scaling is only valid in a saturated case, where the net magnetization is made up from all chains. In a non-saturated case ($B_{\text{res}} < B_{\text{sat}}$) as it can occur in the S-band mode, only chains parallel to the external field are saturated and are therefore responsible for the FMR signal.

An analytical derivation of FMR spectrum is possible, if the properties of magnetic particles exhibit only little variations and if their one-dimensional configuration is well defined. For samples with magnetic particles in different configurations with a complex sum of anisotropy fields, an empirical spectral separation is applied in order to test the presence of chain assemblies. In such an approach a synthetic spectrum for non-aligned particles is generated and then subtracted from the measured spectrum. The remaining spectrum is discussed with respect to uniaxial properties.

3. Results and discussion

3.1. Static magnetization

For *M. gryphiswaldense* at room temperature, the magnetization loop in a magnetic field reveals hysteresis with $B_c = 16.8$ mT and $B_{\text{sat}} \approx 130$ mT (Fig. 1). The M_r/M_s ratio deduced from the respective magnetic moments was 0.45 that is characteristic for magnetosomes in a SSD domain range (Dunlop and Özdemir, 1997). Fischer et al. (2008) showed that the hysteresis properties for cultured *M. gryphiswaldense* are affected by superparamagnetic particles which lower B_c and M_r/M_s . The natural samples showed hysteresis values similar to those of intact MTB, with $M_r/M_s = 0.42 \pm 0.02$, $B_{\text{sat}} \approx 130$ mT, and $B_c = 23.4 \pm 0.5$ mT. The higher B_c compared to the cultured MTB can be due to the absence of superparamagnetic particles and/or slight variation in grain size distribution. The hysteresis parameters indicate that SSD magnetite particles are the predominant magnetic constituent in the natural sample. Hence one criterion for the presence of MTB is fulfilled.

3.2. X and S-band FMR spectroscopy

The X-band FMR spectrum for *M. gryphiswaldense* shows an asymmetric line-shape, where an extended low-field resonance with two distinct peaks and a shoulder was observed. The low-field resonance occurs in fields higher than B_{sat} . The A parameter of this signal is about 0.2, which is indicative for predominate uniaxial anisotropy. The spectral parameters are $B_{\text{res}} = 382.8$ mT, corresponding to $g_{\text{eff}} = 1.83$, and line width $\Delta B = 178.5$ mT. The asymmetry and

the shift of B_{res} to higher fields compared to a single crystal magnetite (Bickford, 1950) are characteristic for a one-dimensional configuration of magnetite particles with predominant uniaxial anisotropy as found in MTB (Fischer et al., 2008; Kopp et al., 2006a; Weiss et al., 2004). The FMR response in the S-band exhibits two separated absorption features. The high field resonance has $B_{\text{res}} = 157.9$ mT with $g_{\text{eff}} = 1.84$, similar to the spectral parameters found in the X-band where $B_{\text{res}} > B_{\text{sat}}$. The absorption in the low-field range occurs in fields less than B_{sat} with $B_{\text{res}} = 36.5$ mT, corresponding to $g_{\text{eff}} = 7.78$. Similar values were found for mature *M. gryphiswaldense* (Faivre et al., 2010). Detailed studies by Mastrogiamomo et al. (2010) showed that the low-field absorption arises from selected magnetosome chains aligned parallel to the sweeping field. Chains that are parallel to the external field are saturated in contrast to those with other orientations. The above results demonstrate that if the MTB are intact and the magnetosome chains are the only magnetic phase in the bulk sample, they can easily be detected by X-band as well as by S-band FMR spectroscopy.

In order to better characterize the anisotropy properties of the intact MTB the model by Charilaou et al. (2011) is applied as described above. As seen in Fig. 3 the simulated spectra reproduce the peak-positions obtained from the measured data for both frequencies. For the numerical treatment of the experimental data the two parameters B_{uni} and B_{cub} are adjusted. The best fit yields value of $B_{\text{uni}} = 96 \pm 1$ mT and $B_{\text{cub}} = 22 \pm 1$ mT, which indicates the predominance of uniaxiality. These values for the anisotropy fields can be used to fit the X- and the S-band spectra with one restriction: for the X-band fit the ensemble of randomly oriented chains is treated statistically using Eq. (2). For the S-band, however, no statistical scaling is performed in order to reconcile for the fact that only chains parallel to the external field are saturated at B_{res} . This shows, in turn, that the presence of intact chains produces the characteristic peak in S-band spectra of such ensembles.

To test the robustness of detecting intact MTB and/or magnetofossils in natural samples, the two-frequency FMR spectroscopy is applied to three samples from lake sediments. Although the X- and S-band measurements exhibit different spectral traits, the spectra obtained from the three samples were similar (Fig. 3). This suggests that the overall anisotropy properties for the three samples can be considered to be the same.

The X-band FMR spectra of the natural samples exhibit only minor absorption in the field range less than B_{sat} of about 130 mT, as deduced from the hysteresis loop (Fig. 1). The absence of zero-field absorption, however, indicates SSD magnetite only, i.e., there is no microwave absorption by domain walls (e.g. Gehring et al., 2009). The spectral parameters $B_{\text{res}} = 349.6 \pm 15.9$ mT corresponds to $g_{\text{eff}} = 2.02 \pm 0.01$, and $\Delta B = 207.5 \pm 20.1$ mT. Considering the g_{eff} of 2.11 obtained from a single magnetite crystal magnetized along the [111] easy axis (Bickford, 1950), g_{eff} measured for the lake sediments are in between the values for cultured *M. gryphiswaldense* magnetosome chains and magnetite with no shape anisotropy. The $A = 0.62 \pm 0.01$ suggests uniaxial anisotropy in the samples, but it is markedly lower than the one for *M. gryphiswaldense* with its strong cellular magnetic dipole resulting in $A = 0.2$. The lesser development of uniaxiality is probably the result of diagenetic processes by which cytoskeletal protein filaments, that stabilize the alignment of magnetosomes, become decomposed. The strong cellular dipole in *M. gryphiswaldense* bacteria yields to a clearly defined low-field resonance in the S-band spectrum (Fig. 2). The spectra found for the natural sample exhibit no clear absorption in the low field range (Fig. 3). In the high field range at $g_{\text{eff}} < 2$, where the sample is saturated, the spectral response of X- and S-band are similar as indicated by the ratio about 1 of the high-field absorption ΔB_{high} obtained at the two frequencies. The absence of the clear low-field resonance in the S-band and its detection in the X-band suggest that the different response is caused by the magnetization status of the sample. By contrast to the X-band, in the S-band measurements magnetite is far from saturation in

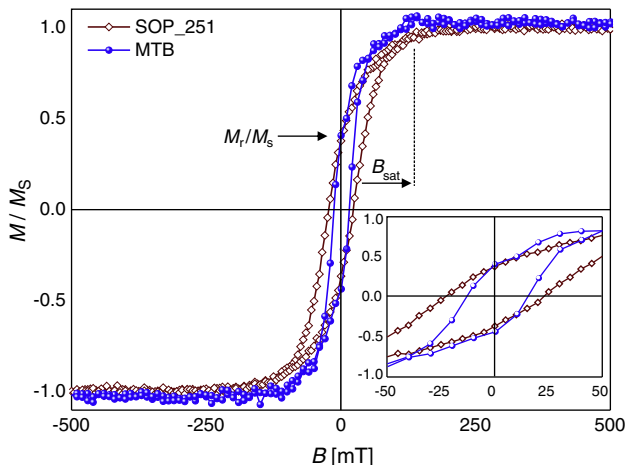


Fig. 1. Normalized hysteresis loops of intact MTB (dots) and natural sample SOP_251 (diamonds) with inset shows a blow-up the central part of the loop.

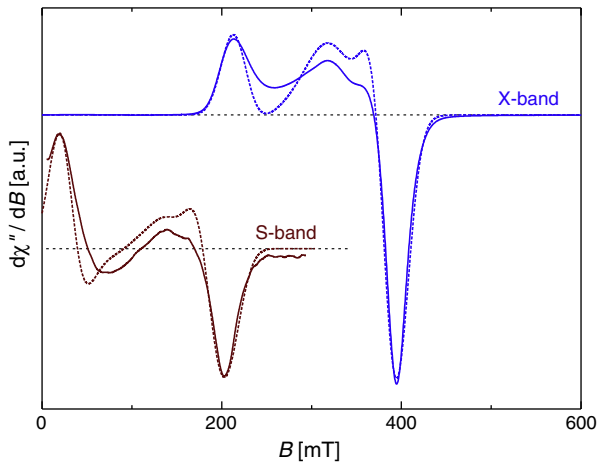


Fig. 2. X- and S-band FMR spectra of intact MTB chains. Dotted lines correspond to calculated fits using the model by Charilaou et al. (2011).

the low field range (Fig. 3). The absence of resonance in the sediment samples could be due to the lack of intact chains and/or the occurrence of magnetite in different assemblies such as clumps or chain fragments, which could create a heterogeneous internal field in the assay.

It can be expected that the FMR response from lake sediments contains spectral contributions from different configurations of magnetic particles. Because of the spectral superposition, an analytical derivation of the FMR signals with defined B_{uni} and B_{cub} as shown for the cultured MTB, is not possible for the natural sample. In order to deduce configurations of the magnetite particles in the sediment samples, an empirical spectral separation approach is used to infer different contributions to the X-band spectra. A similar approach was reported by Maloof et al. (2007) to infer different magnetic components in a sedimentary deposit. For our straightforward approach, it is assumed that the morphology of the magnetite is approximately spherical and there is no critical variation of the particle size. This assumption is in good agreement with $B_c \approx 23$ mT, which is close to the theoretical value for spherical SSD particles (Dunlop and Özdemir, 1997). Considering distinct elongated SSD particles, as reported for different wild-type MTB, B_c is expected to be higher (Stacey and Banerjee, 1974) and a FMR spectral response would become more asymmetric (Valstyn et al., 1962). For simplicity, two configurations of SSD particles are supposed to occur in the sediment samples. One contains magnetite that forms chains or chain-like assemblies, and the other is made up of dissociated magnetite that is randomly distributed. The latter can contain SSD particles that were formed by inorganic or biologically-induced

processes or they are remains of magnetosome chains (e.g. Egli et al., 2010). It is known that the FMR responses of such two populations differ in their g_{eff} and A values (Fischer et al., 2008; Kopp et al., 2006b; Valstyn et al., 1962). For the dissociated particles a spectrum with nearly symmetric Lorentzian shape is taken. The FMR response of the second population is deduced by the subtraction of the Lorentzian component from the measured spectrum. A physically meaningful solution is obtained, if the randomly distributed magnetite generates a signal with $g_{\text{eff}} = 2.25$ and $A \approx 1$, superimposed by a signal with $g_{\text{eff}} = 1.91$ and $A < 1$ (Fig. 4). In this case the latter exhibits two peaks in the low-field range similar to those observed for intact MTB (Fig. 2). Based on FMR parameters Kopp et al. (2006a) introduced an empirical discrimination parameter α ($\alpha = 0.17A + 9.8 \times 10^{-4} \Delta B/\text{mT}$) to infer MTB and magnetofossils. Cultured MTB have typically $\alpha < 0.25$ and magnetofossils $\alpha < 0.3$. These values agree well with the findings in the present study, where the intact MTB have an $\alpha = 0.2$ and lake sediments have an $\alpha = 0.3$. The $\alpha \approx 0.25$ for the separate spectra is indicative of magnetofossils (Kopp et al., 2007).

The absence of the low field resonance in the S-band and the two features in the low-field range in the X-band suggests that these magnetofossils are mainly preserved as chain fragments. Although the magnetization which determines the FMR signal intensity is unknown, it can be inferred from the separated spectra, that the magnetic information in the sediment samples is substantially carried by magnetofossils.

4. Conclusion

Anisotropy that originates from cellular magnetic dipoles due to magnetite chains is a critical property for the unambiguous detection of MTB and their fossil remains. The decay of cellular matter during diagenesis disintegrates chain assemblies, resulting in chain fragments and/or randomly distributed SSD magnetite particles that are generally preserved in sedimentary deposits. The FMR spectroscopy of Holocene lake sediments clearly demonstrates that SSD magnetite particles occur both as randomly distributed particles and as chain fragments with a pronounced uniaxial anisotropy. This demonstrates the strong potential of two-frequency FMR spectroscopy for detecting magnetofossils that is a prerequisite for a better insight into the microbial evolution during Earth's history.

Acknowledgments

The authors thank J. Warthmann for preparing the MTB, Susan Glasauer, Bill Lowrie, and Michael Winklhofer for critical discussion of the

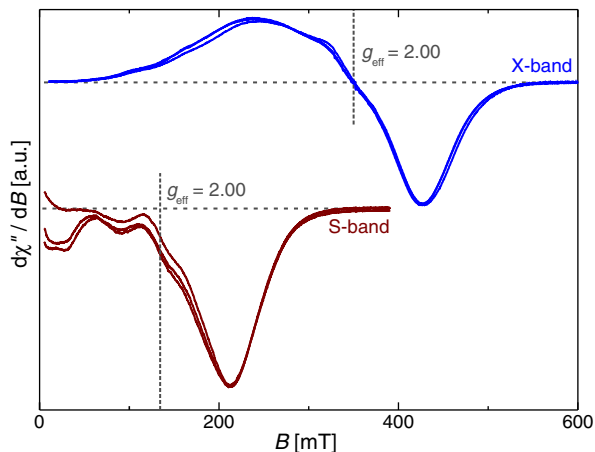


Fig. 3. Superposition of normalized X- and S-band FMR spectra of the samples SOP_251, SOP_258, and SOP_264. The positions of $g_{\text{eff}} = 2.00$ are indicated as reference.

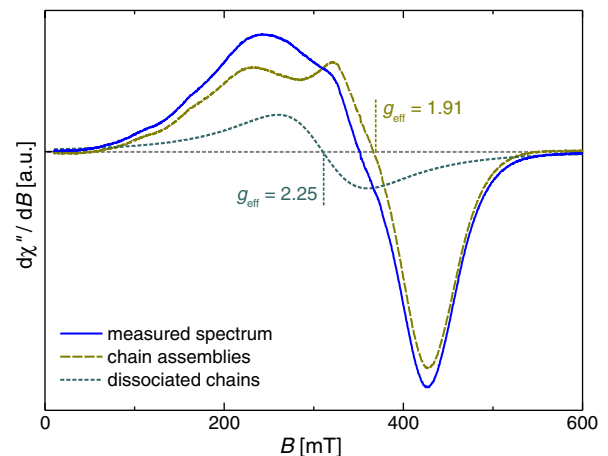


Fig. 4. Empirical spectral separation of the FMR spectrum yields from SOP_251.

manuscript. The research was financially supported by the Swiss National Science Foundation (Grant no. 121844) and CHIRP1 project of ETH Zurich.

References

- Bazylinski, D.A., Frankel, R.B., 2004. Magnetosome formation in prokaryotes. *Nat. Rev. Microbiol.* 2, 217–230.
- Bickford, L.R., 1950. Ferromagnetic absorption in magnetite single crystals. *Phys. Rev.* 78, 449–457.
- Blakemore, R.B., 1975. Magnetotactic bacteria. *Science* 190, 377–379.
- Charilaou, M., Winklhofer, M., Gehring, A.U., 2011. Simulation of ferromagnetic resonance spectra of linear chains of magnetite nano-crystals. *J. Appl. Phys.* 109, 093903. doi:10.1063/1.3581103.
- Devouard, B., Posfai, M., Hua, X., Bazylinski, D.A., Frankel, R.B., Buseck, P.R., 1998. Magnetite from magnetotactic bacteria: size distributions and twinning. *Am. Mineralog.* 83, 1387–1398.
- Dunin-Borkowski, R.E., McCartney, M.R., Frankel, R.B., Bazylinski, D.A., Pósfai, M., Buseck, P.R., 1998. Magnetic microstructure of magnetotactic bacteria by electron holography. *Science* 282, 1868–1870.
- Dunlop, D.J., Özdemir, Ö., 1997. *Rock Magnetism: Fundamentals and Frontiers*. Cambridge Univ Press.
- Egli, R., Chen, A.P., Winklhofer, M., Kodama, K.P., Horng, C.S., 2010. Detection of noninteracting single domain particles using first-order reversal curve diagrams Q01Z11 *Geochim. Geophys. Geosyst.* 11. doi:10.1029/2009GC002916.
- Faivre, D., Fischer, A., Mastrogiacomio, G., García-Rubio, I., Gehring, A.U., 2010. Development of cellular magnetic dipoles in magnetotactic bacteria. *Biophys. J.* 99, 1268–1273.
- Fischer, A., 1996. *Isotopenchemische Untersuchung ($\delta^{18}\text{O}$ und $\delta^{13}\text{C}$) im Wasser und in den Sedimenten des Soppensees (Kt. Luzern, Schweiz)*. PhD Thesis no. 11924, ETH Zurich, 184pp.
- Fischer, H., Mastrogiacomio, G., Löffler, J.F., Warthmann, R.J., Weidler, P.G., Gehring, A.U., 2008. Ferromagnetic resonance and magnetic characteristics of intact magnetosome chains in *Magnetospirillum gryphiswaldense*. *Earth Planet. Sci. Lett.* 270, 200–208.
- Frankel, R.B., Blakemore, R.P., Wolfe, R.S., 1979. Magnetite in freshwater magnetotactic bacteria. *Science* 203, 1355–1356.
- Gehring, A.U., Fischer, H., Louvel, M., Kunze, K., Weidler, P.G., 2009. High temperature stability of natural maghemite: a magnetic and spectroscopic study. *Geophys. J. Int.* 179, 1361–1371.
- Hesse, P.P., 1994. Evidence for bacterial paleoecological origin of mineral magnetic cycles in oxic and sub-oxic Tasman Sea sediments. *Mar. Geol.* 117, 1–17.
- Heyen, U., Schüler, D., 2003. Growth and magnetosome formation by microaerophilic *Magnetospirillum* strains in an oxygen-controlled fermentor. *Appl. Microbiol. Biotechnol.* 61, 536–544.
- Jimenez-Lopez, C., Romanek, C.S., Bazylinski, D.A., 2010. Magnetite as a prokaryotic biomarker: a review G00G03 *J. Geophys. Res.* 115. doi:10.1029/2009JG001152.
- Kopp, R.E., Kirschvink, J.L., 2008. The identification and biochemical interpretation of fossil magnetotactic bacteria. *Earth Sci. Rev.* 86, 42–61.
- Kopp, R.E., Weiss, B.P., Maloof, A., Vali, H., Nash, C.Z., Kirschvink, J.L., 2006a. Chains, clumps, and strings: magnetofossil taphonomy with ferromagnetic resonance spectroscopy. *Earth Planet. Sci. Lett.* 247, 10–25.
- Kopp, R.E., Nash, C.Z., Kobayashi, A., Weiss, B.P., Bazylinski, D.A., Kirschvink, J.L., 2006b. Ferromagnetic resonance spectroscopy for assessment of magnetic anisotropy and magnetostatic interactions: a case study of mutant magnetotactic bacteria B12S25 *J. Geophys. Res.* 111. doi:10.1029/2006JB004529.
- Kopp, R.E., Raub, T.D., Schumann, D., Vali, H., Smirnov, A.V., Kirschvink, J.L., 2007. Magnetofossils spike during the Paleocene-Eocene thermal maximum: ferromagnetic resonance, rock magnetic, and electron microscopy evidence from Ancora, New Jersey, United States PA4103 *Paleoceanography* 22. doi:10.1029/2007PA001473.
- Lotter, A., 2001. The paleolimnology of Soppensee (Central Switzerland) as evidenced by diatoms, pollen, and fossil-pigment analyses. *J. Paleolimnol.* 25, 65–79.
- Maloof, A., Kopp, Grotzinger, J.P., Fike, D.A., Bosak, T., Vali, H., Poussart, P.M., Weiss, B.P., Kirschvink, J.L., 2007. Sedimentary iron cycling and the origin and preservation of magnetization in platform carbonate muds, Andros Island, Bahamas. *Earth Planet. Sci. Lett.* 259, 581–598.
- Mann, S., Sparks, N.H.C., Blakemore, R.P., 1987. Ultrastructure and characterization of anisotropic magnetite inclusions in magnetotactic bacteria. *Proc. R. Soc. Lond. B* 231, 469–476.
- Mastrogiacomio, G., Fischer, H., García-Rubio, I., Gehring, A.U., 2010. Ferromagnetic resonance spectroscopic response of magnetite chains in a biological matrix. *J. Magn. Magn. Mater.* 332, 661–663.
- McNeill, D.F., Kirschvink, J.L., 1993. Early dolomitization of platform carbonates and the preservation of magnetic polarity. *J. Geophys. Res.* 98, 7977–7986.
- Muxworthy, A.R., Williams, W., 2009. Critical superparamagnetic/single-domain grain sizes in interacting magnetite particles: implications for magnetosome crystals. *J. R. Soc. Interface* 6, 1207–1212.
- Philippe, A.P., Maas, D., 2002. Magnetic Colloids from magnetotactic bacteria: chain formation and colloidal stability. *Langmuir* 18, 9977–9984.
- Scheffel, A., Gruska, M., Faivre, D., Linaoudis, A., Plitzko, J.M., Schüler, D., 2006. An acidic protein aligns magnetosomes along a filamentous structure in magnetotactic bacteria. *Nature* 440, 110–114.
- Snowball, I., 1994. Bacterial magnetite and magnetic properties of sediments in a Swedish lake. *Earth Planet. Sci. Lett.* 126, 129–142.
- Snowball, I., Sandgren, P., 2004. Geomagnetic field intensity changes in Sweden between 9000 and 450 cal BP: extending the record of “archaeomagnetic jerks” by means of lake sediments and the pseudo-Thellier technique. *Earth Planet. Sci. Lett.* 227, 361–376.
- Stacey, F.D., Banerjee, S.K., 1974. *The Physical Principles of Rock Magnetism*. Elsevier, New York.
- Valstyn, E.P., Hanton, J.P., Morrish, A.H., 1962. Ferromagnetic resonance of single-domain particles. *Phys. Rev.* 128, 2078–2087.
- Ferromagnetic Resonance. In: Vonsovskii, S.V. (Ed.), Pergamon Press Oxford.
- Watanabe, S., Akutagawa, S., Sawada, K., Iwasa, T., Shimoyama, Y., 2009. A ferromagnetic resonance study of iron complexes as biologically synthesized in magnetic bacteria. *Mater. Trans.* 9, 2187–2191.
- Weiss, B.P., Kim, S.S., Kirschvink, J.L., Kopp, R.E., Sankaran, M., Kobayashi, A., Komeili, A., 2004. Ferromagnetic resonance and low-temperature magnetic test for biogenic magnetite. *Earth Planet. Sci. Lett.* 224, 73–89.
- Zhang, Y., Sun, L., Fu, Y., Huang, Z.C., Bai, X.J., Zhai, Y., Du, J., Zhai, H.R., 2009. The shape anisotropy in the magnetic field-assisted self-assembly chain-like structure of magnetite. *J. Phys. Chem. C* 113, 8152–8157.